Supporting Information
Anisotropic luminophore emission for enhanced light trapping in luminescent solar concentrator waveguides

Tom Veeken[a,*], Kyra Orbons[a], Nelson de Gaay Fortman[a], Aurelio A. Rossinelli[b], David J. Norris[b], A. Femius Koenderink[a], and Albert Polman[a]

[*]Corresponding author, t.veeken@amolf.nl

[a]NWO-Institute AMOLF, Science Park 104, 1098 XG Amsterdam, the Netherlands
[b]Optical Materials Engineering Laboratory, Department of Mechanical and Process Engineering, ETH Zurich, 8092 Zurich, Switzerland

Downloaded from pubs.acs.org/aamick/article-supplement/5221134/pdf/am-2025-210664_si_001/ by AMOLF user on 12 August 2026

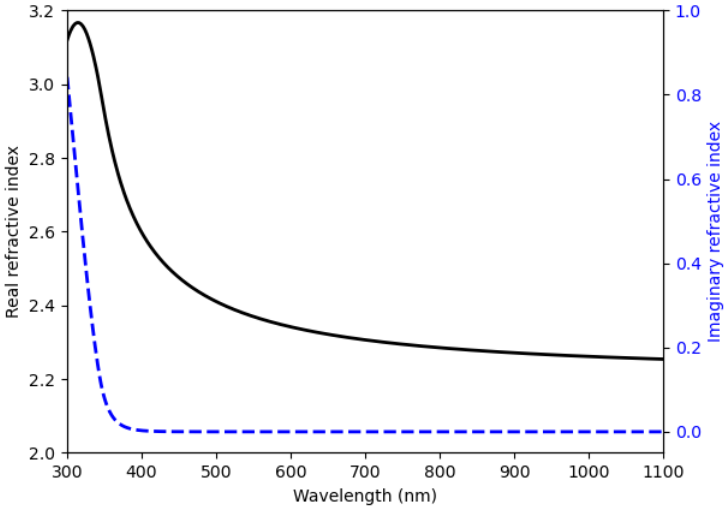

Figure S1: *Real (black) and imaginary (blue dashed) parts of the refractive index of a TiO_2 thin film as fitted from ellipsometry measurements. A Cody-Lorentz oscillator model was used, yielding a mean squared error (MSE) of 4.*

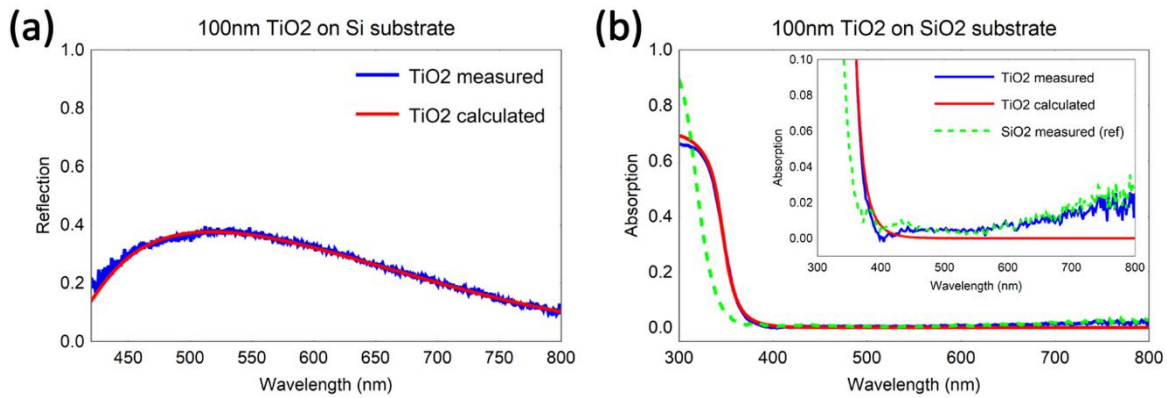

Figure S2: *(a) Reflection and (b) absorption by a 100 nm TiO_2 thin film on a silicon (glass) substrate, measured in an integrating sphere setup and calculated using the n,k values obtained from ellipsometry. The excellent agreement corroborates the fitted values. The nonzero absorption for longer wavelengths is attributed to scattering by the glass substrate. The TiO_2 thin film was evaporated with EBPVD on the silicon and glass substrates simultaneously.*

Downloaded from pubs.acs.org/aamick/article-supplement/5221134/pdf/am-2025-210664_si_001/ by AMOLF user on 12 August 2026

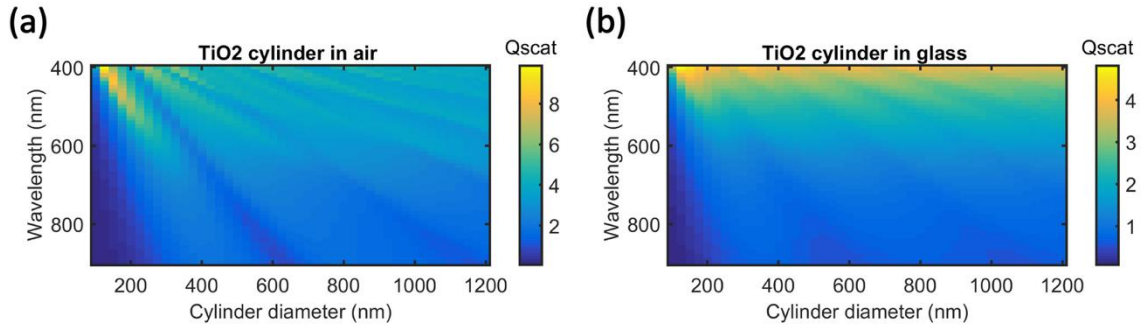

Figure S3: *Calculated, normalized scattering cross (Qscat, color scale) as a function of wavelength and cylinder diameter for a cylinder in air (a) and a cylinder in glass (b). Qscat is calculated using FDTD simulations and defined as the scattering cross-section normalized to geometrical cross-section for a normal-incident plane wave. The diagonal interference patterns indicate the presence of Mie-like resonances. The Mie-like resonances are more prominent in the left graph due to the larger refractive index contrast between air and TiO_2.*

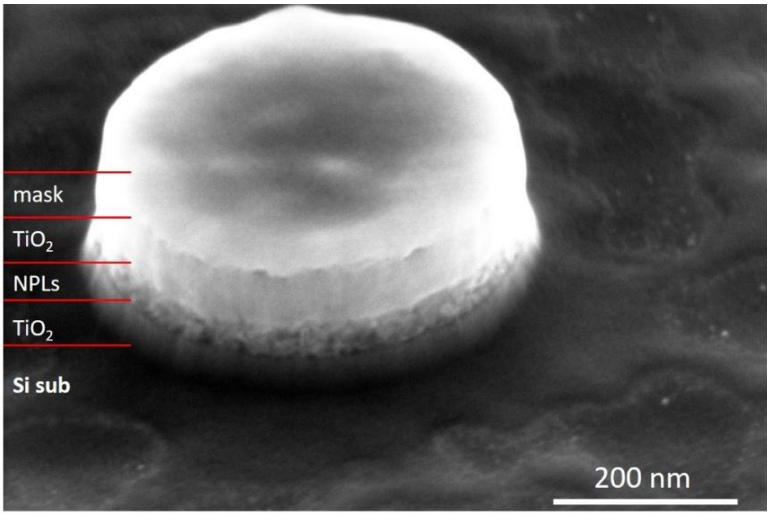

Figure S4: *Scanning electron microscopy (SEM) image of a TiO_2 nanocylinder with embedded semiconductor nanoplatelets (NPLs), fabricated for reference on a silicon substrate. The image is taken under a 45-degree angle. The silicon substrate facilitates charge dissipation in the SEM, avoiding sample charging. In contrast to the homogeneous TiO_2 layer on top, the NPL layer shows many features on its surface. The ma-N e-beam resist mask is still on top of the cylinder.*

Downloaded from pubs.acs.org/aamick/article-supplement/5221134/pdf/am-2025-210664_si_001/ by AMOLF user on 12 August 2026

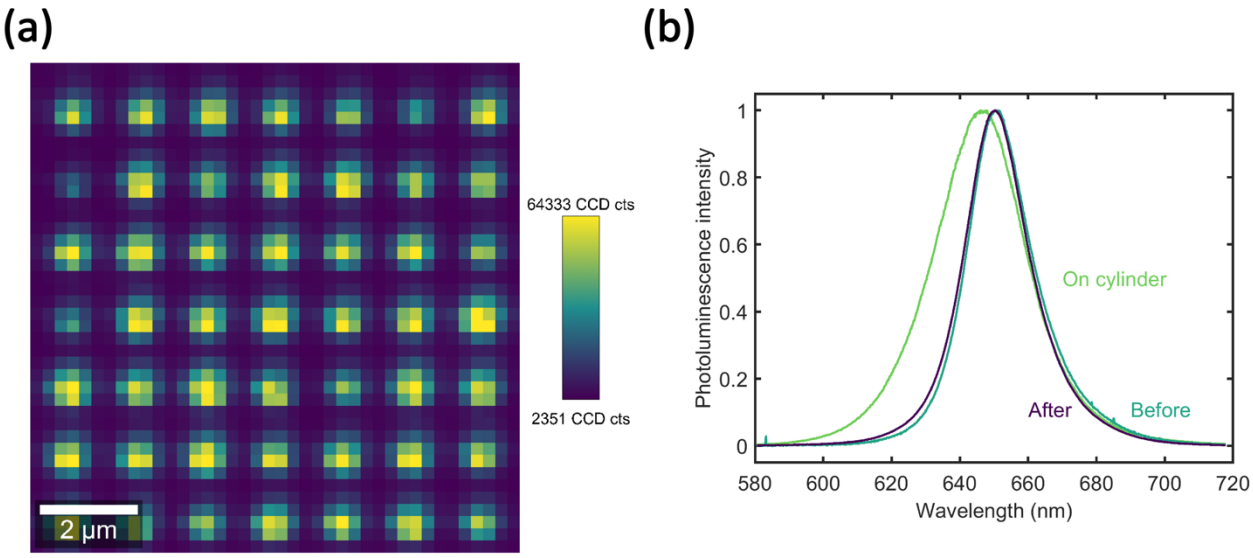

Figure S5: *(a) Identical to the data presented in Fig. 4b, but without smoothing the data: Photoluminescence intensity map of the marked area in Fig. 4a, indicating emission is confined to the nanocylinders. Color scale depicts the intensity at the target wavelength of 650 nm, in counts per pixel, for 1 mW input power of the 532 nm CW laser and 100 ms CCD integration time. A background level of 535 counts was subtracted. (b) Photoluminescence spectra of the CdSe-CdZnS core-shell nanoplatelet layer during different steps in the fabrication process. The two nearly overlapping curves correspond to photoluminescence from the nanoplatelet layer on top of the first TiO_2 layer before deposition (green) and after deposition of the second TiO_2 layer (purple). The green curve shows the same photoluminescence data as shown in Figure 4c corresponding to the final nanocylinder array sample. Clearly, the photoluminescence spectrum is not influenced by the deposition of the second TiO2 layer and corresponds to the reported spectrum for these nanoplatelets in ref [59]: 655 nm peak wavelength and 19.5 nm FWHM. The introduction of the nanocylinder array does slightly change the spectrum, blue-shifting the peak and broadening towards the blue.*

Downloaded from pubs.acs.org/aamick/article-supplement/5221134/pdf/am-2025-210664_si_001/ by AMOLF user on 12 August 2026

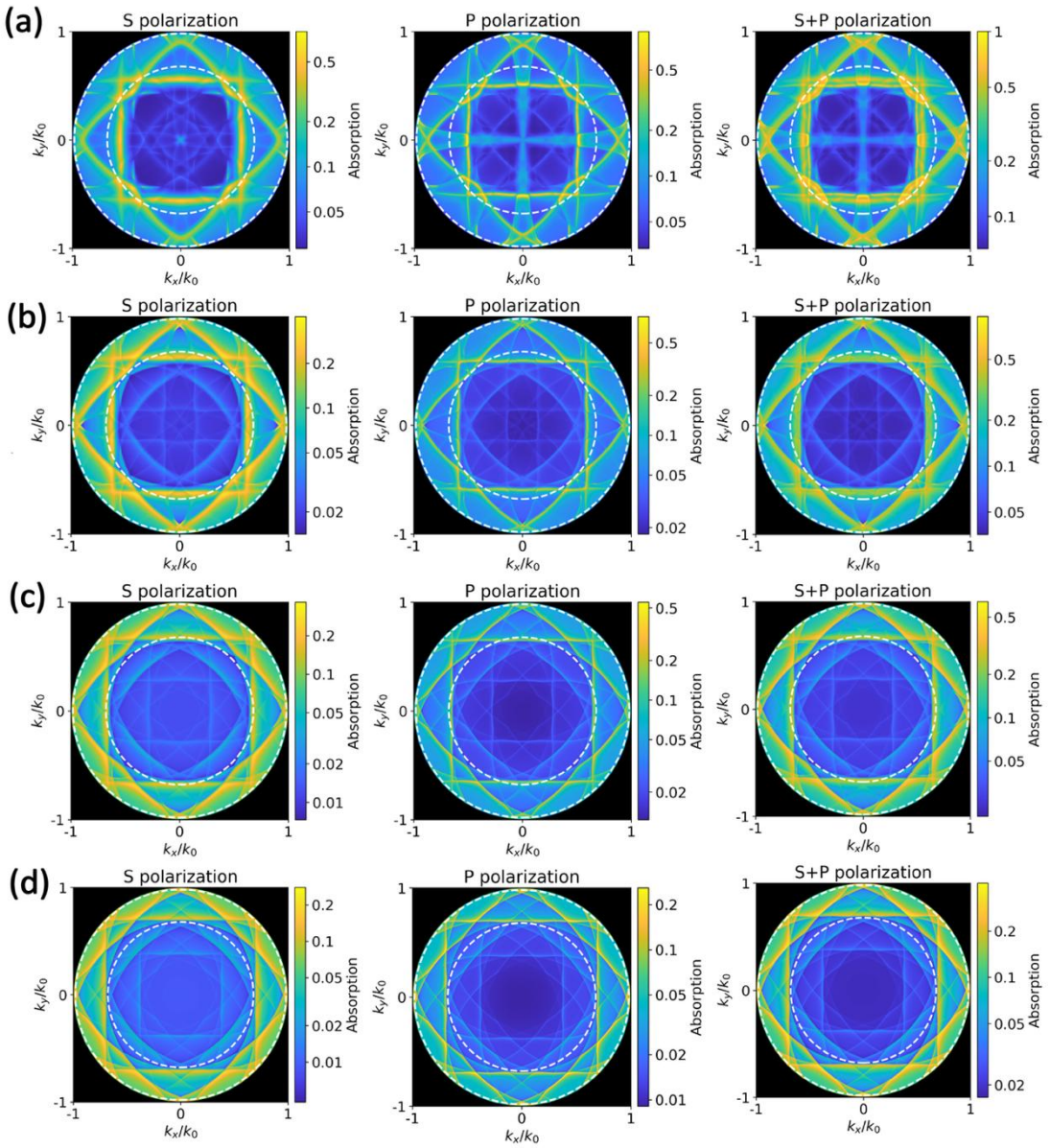

Figure S6: *Angle-resolved photoluminescence simulated for a (a) 800 nm, (b) 1000 nm, (c) 1200 nm, and (d) 1400 nm pitch array. The left and middle plots on each row correspond to the s and p polarization, whereas the right plot shows the averaged polarization, identical to the simulated plots in Figure 5 of the main text. The white dashed lines correspond to NA = 1 (critical angle from glass substrate to air) and NA = 1.45 (maximum for the objective).*

Downloaded from pubs.acs.org/aamick/article-supplement/5221134/pdf/am-2025-210664_si_001/ by AMOLF user on 12 August 2026

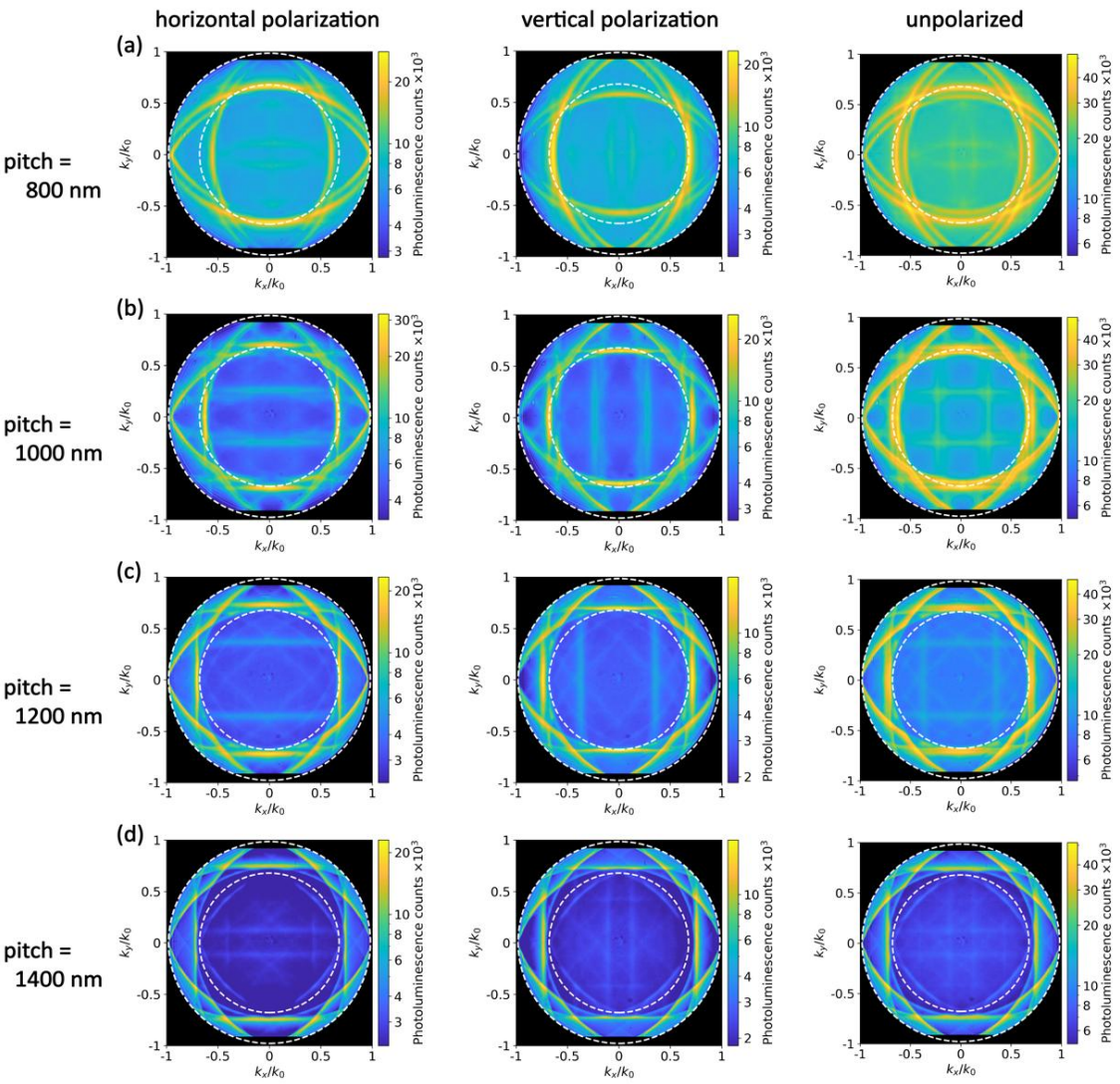

Figure S7: *Angle-resolved photoluminescence measured on a (a) 800 nm, (b) 1000 nm, (c) 1200 nm, and (d) 1400 nm pitch array. The left and middle plots on each row correspond to the horizontal and vertical polarization, whereas the right plot shows the averaged polarization, identical to the measured plots in Figure 5 of the main text. The white dashed lines correspond to NA = 1 (critical angle from glass substrate to air) and NA = 1.45 (maximum for the objective).*

Downloaded from pubs.acs.org/aamick/article-supplement/5221134/pdf/am-2025-210664_si_001/ by AMOLF user on 12 August 2026

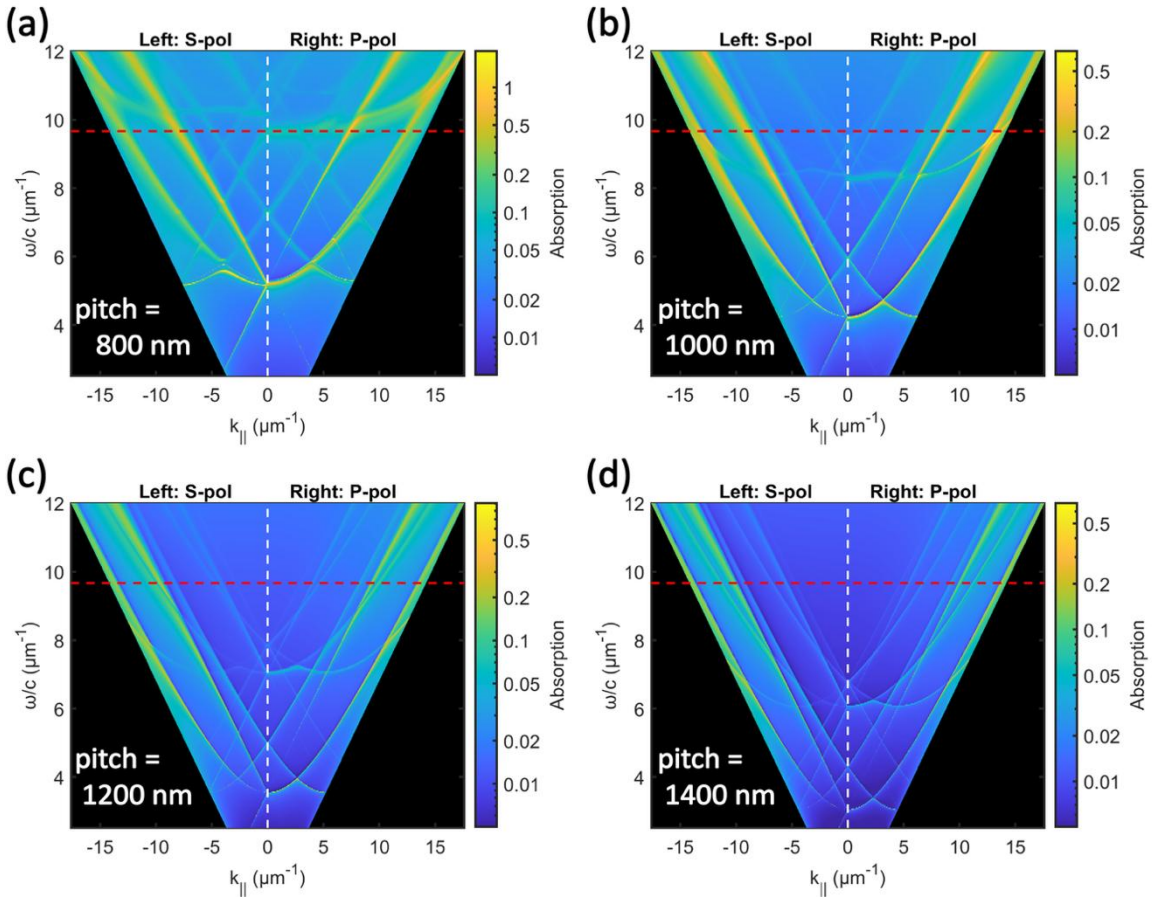

***Figure S8**. Calculated dispersion diagrams for a (a) 800 nm, (b) 1000 nm, (c) 1200 nm, and (d) 1400 nm pitch array. The left and right sides of the graphs show the s and p polarized emission, along the $k_{par} = k_x$ axis and as a function of normalized frequency ($2\pi/\lambda$). The white dashed line indicates the border between the s and p polarized data. The red dashed line indicates the target wavelength of 650 nm, corresponding to a horizontal cut through the plots in Figure S6 at $k_y = 0$. As we already observed in Figures 5 and S6, the photonic crystal bands are displaced outwards with increasing array pitch.*

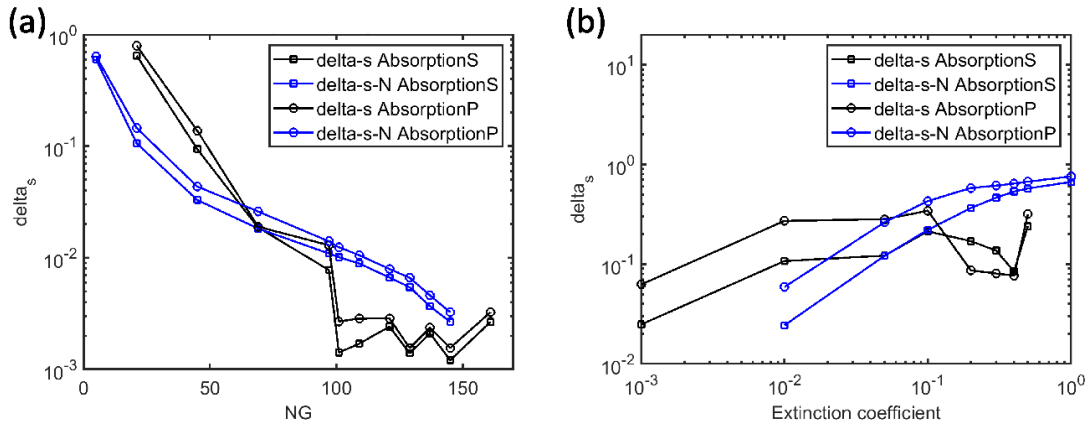

***Figure S9**. S^4 calculation convergence testing for (a) the number of Fourier series components (NG) and (b) the extinction coefficient (Im(ε)) of the absorbing center layer. Convergence was found at NG = 101, which is used in the extinction simulations, where convergence was found for Im(ε) = 0.1. See Methods section for definition of Δσ (delta-s) and $\Delta\sigma_N$ (delta-s-N).*

Downloaded from pubs.acs.org/aamick/article-supplement/5221134/pdf/am-2025-210664_si_001/ by AMOLF user on 12 August 2026